

From Soft to Adaptive Synergies: the Pisa/IIT SoftHand

M. G. Catalano^{1,2}, G. Grioli^{1,2}, E. Farnioli^{1,2}, A. Serio², M. Bonilla², M. Garabini², C. Piazza², M. Gabbicini^{1,2}, A. Bicchi^{1,2}

Abstract Taking inspiration from the neuroscientific findings on hand synergies discussed in the first part of the book, in this Chapter we present the Pisa/IIT SoftHand, a novel robot hand prototype. The design moves under the guidelines of making an hardware robust and easy to control, preserving an high level of grasping capabilities and an aspect as similar as possible to the human counterpart. First, the main theoretical tools used to enable such simplification are presented, as for example the notion of *soft synergies*. A discussion of some possible actuation schemes shows that a straightforward implementation of the soft synergy idea in an effective design is not trivial. The proposed approach, called *adaptive synergy*, rests on ideas coming from underactuated hand design, offering a design method to implement the desired set of soft synergies as demonstrated both with simulations and experiments. As a particular instance of application of the synthesis method of adaptive synergies, the Pisa/IIT SoftHand is described in detail. The hand has 19 joints, but only uses one actuator to activate its adaptive synergy. Of particular relevance in its design is the very soft and safe, yet powerful and extremely robust structure, obtained through the use of innovative articulations and ligaments replacing conventional joint design. Moreover, in this work, summarizing results presented in previous papers, a discussion is presented about how a new set of possibilities is open from paradigm shift in manipulation approaches, moving from manipulation with rigid to soft hands.

¹Istituto Italiano di Tecnologia, Department of Advanced Robotics, Via Morego 30, 16163, Genova, Italy,

e-mail: {m.catalano, g.grioli, e.farnioli, m.gabbicini, a.bicchi}@iit.it.

²Università di Pisa, Research Center E. Piaggio, Largo Lucio Lazzarino 1, 56122, Pisa, Italy, e-mail: {a.serio, m.bonilla, c.piazza, m.garabini}@centropiaggio.unipi.it.

1 Introduction

In the first part of the book, the neuroscientific concept of hand synergies, i.e. motor primitives or common actuation patterns of neuro-muscular activities for the human hand, has been widely discussed and considered at different levels (neural, muscular, kinematic and sensory, see Chapters 1-6).



Fig. 1: Skeleton of the Pisa/IIT SoftHand advanced anthropomorphic hand prototype implementing one adaptive synergy. The prototype dimensions are comparable to those of the hand of an adult human.

Recently, different approaches in robotics tried to take advantage from the idea of synergies, aiming to reproduce a similar “coordinated and ordered ensemble” of human hand motions. To transfer part of the embodied intelligence, typical of the human hand, into a robotic counterpart, a promising possibility is the re-creation of synergy patterns as a feature of the mechatronic hand system. This approach has already been tried in recent literature (see next section for a short review), although a purely kinematic model of synergies leads to inconsistent grasp force distribution models. To solve such problems, the concept of *soft synergies* was introduced [1, 2], which provides a model of how synergies may generate and control the internal forces needed to hold an object.

In this Chapter, we summarize the results discussed in [3], [4] and [5], presenting how soft synergy idea can be exploited to build robot hands, such as the Pisa/IIT SoftHand, that can grasp a large variety of objects in a stable way, while remaining very simple and robust. Moreover, we show that the Pisa/IIT SoftHand can afford grasping capabilities that are comparable to natural one. Through the observation of human-directed operations of the prototype it appears how fundamental in everyday grasping and manipulation is the role of hand compliance. Indeed, the Pisa/IIT SoftHand can be functionally shaped using both the object to grasp and

the environmental constraints, going beyond nominal kinematic limits by suitably exploiting its structural softness.

The approach to the principled simplification of hand design can be summarized as follows. From statistical observations of human grasping, we derive the hand postures most often used in the grasp approach phase (aka synergies, see also Chapters 1, 2, 4) and a mathematical description on the basis of the soft synergy model (see also Chapters 11 and 12). Indeed, as also discussed in Chapter 8, human-like hand movement has great influence in the possibility of successfully achieving a large number of grasps belonging to the sphere of activities of daily living (ADL). The actual realization of the hand mechanics is not however a straightforward implementation of the soft synergy model. Indeed, to achieve a simple and compact design and better robustness, we recur to the technology of underactuated hands [6], complementing it with innovative joint and ligament design. A relevant point discussed in this work regards how the design parameters of an underactuated hand can be chosen so that its motion replicates a given set of synergies, in a sense allowing the translation of the concept of *soft synergies* into *adaptive synergies*.

The result of our design method is the Pisa/IIT SoftHand (see fig. 1), a 19-joint hand with anthropomorphic features, which grasps objects of rather general shape by using only a single actuator, and employing an innovative design of articulations and ligaments, which provides a high degree of compliance to external solicitations.

The Chapter is organized as follows: Section 2 briefly presents the analytical model of grasping problem for fully actuated hand and underactuated hands, both via soft and adaptive synergies. Section 3 describes in detail the architecture of the Pisa/IIT SoftHand and Section 4 presents the grasping results experimentally obtained. Section 5 addresses the issue of the change of paradigm in the problem of grasping with SoftHands, i.e. compliant yet robust robotic hands. Finally, conclusions are drawn in Section 6.

2 Hand Actuation, Synergies and Adaptation

2.1 Fully Actuated Hands

In this Section, we briefly present a description of the principal actuation paradigms for the design of robotic systems. The nomenclature and notation are synthesized in Table 1. Finally, we present a map between the human inspired *soft synergy* model (see also Chapter 12) and the *adaptive synergy* design used in the Pisa/IIT SoftHand. More theoretical details about grasp analysis are presented in Chapters 11 and 12 and in [7], [8], and [9].

Starting from fully actuated hands, a quasi-static description of the problem of object grasping can be formalized through a system of three equations as

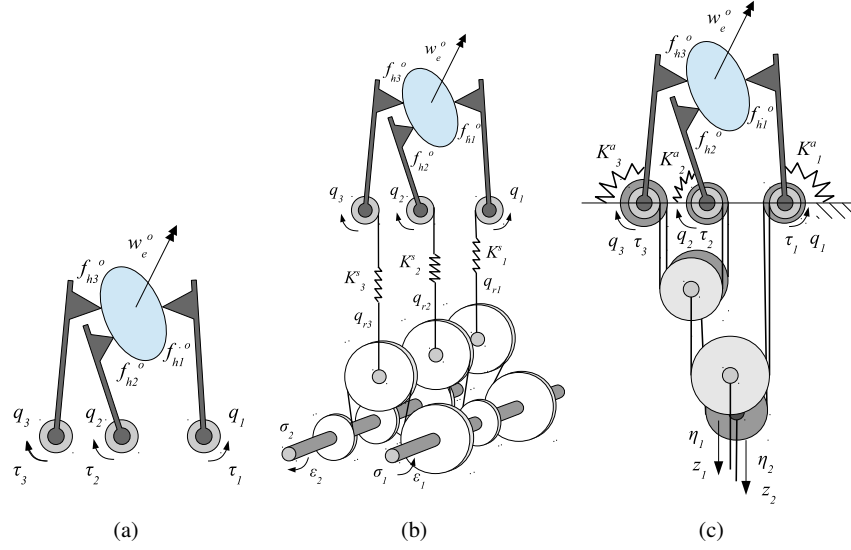


Fig. 2: A simple hand grasping an object with different types of (under)actuation. More in detail, panel (a) shows a conceptual schematics of a simple bi-dimensional fully actuated hand grasping an object. Panel (b) shows the Soft Synergy Actuation scheme applied to the same hand. Panel (c) shows two adaptive synergies used for the underactuation mechanism.

$$\delta w + G\delta f_c = 0, \quad (1)$$

$$\delta \tau = Q\delta q + U\delta u + J^T \delta f_c, \quad (2)$$

$$\delta f_c = K_c(J\delta q - G^T \delta u). \quad (3)$$

More specifically, the object equilibrium equation, in (1), establishes a relationship between external disturbances acting on the object and contact forces that the hand exerts on the object; eq. (2) describes the joint torque variation required to compensate contact force variation and/or kinematic displacement of the system, and the contact constitutive equation (3) relates contact force variation with the mutual displacements of the hand and the object contact points.

More in detail, in equation (1), the symbol $w \in \mathbb{R}^6$ indicates the external wrench acting on the object, described in a local frame $\{O\}$, while $f_c \in \mathbb{R}^c$ are the forces that the hand exerts on the object, described in local contact frames, fixed to the object. The value of c , for the contact force vector, depends on the number and type of contact constraints. For example, a *hard finger* contact, allows the presence of three components of forces, thus it contributes three. The *soft finger* contact, with respect to the hard one, adds the possibility to exert a moment around the normal vector to the contact surface, thus it contributes four. Through the introduction of the *grasp matrix* $G \in \mathbb{R}^{6 \times c}$, the object equilibrium condition is written as

Notation	Definition
δx	variation of variable x
\bar{x}	value of x in the reference configuration
$\#x$	dimension of vector x
$w \in \mathbb{R}^6$	external wrench acting on the object
$u \in \mathbb{R}^6$	pose of the object frame
$f_c \in \mathbb{R}^c$	contact forces exerted by the hand on the object
c	number of contact constraints
$\tau \in \mathbb{R}^{\#q}$	joint torque
$q \in \mathbb{R}^{\#q}$	joint configuration
$q_r \in \mathbb{R}^{\#q}$	reference joint configuration
$\sigma \in \mathbb{R}^{\#\sigma}$	soft synergy configuration
$\varepsilon \in \mathbb{R}^{\#\sigma}$	soft synergy forces
$z \in \mathbb{R}^{\#z}$	adaptive synergy configuration
$\eta \in \mathbb{R}^{\#z}$	adaptive synergy forces
$G \in \mathbb{R}^{6 \times c}$	grasp matrix in object frame
$J \in \mathbb{R}^{c \times \#q}$	hand Jacobian matrix in object frame
$S \in \mathbb{R}^{\#q \times \#\sigma}$	soft synergy matrix
$A \in \mathbb{R}^{\#z \times \#q}$	adaptive synergy matrix

Table 1: Notation for Grasp Analysis.

$$w + Gf_c = 0. \quad (4)$$

Because the equation is written in a reference frame attached to the object, the grasp matrix is constant, hence by differentiating (4), (1) follows.

The hand equilibrium equation relates contact forces with joint torques, $\tau \in \mathbb{R}^{\#q}$, through the transpose of the hand Jacobian matrix $J^T \in \mathbb{R}^{\#q \times c}$, as

$$\tau = J^T f_c. \quad (5)$$

It is worth observing that the Jacobian matrix is here a function both of the hand configuration q and of the object configuration $u \in \mathbb{R}^6$. This is a consequence of the choice to describe the contact interaction in a local frame attached to the grasped object. From this fact it follows that, differentiating (5), (2) is obtained, where the terms $Q = \frac{\partial J^T f_c}{\partial q} \in \mathbb{R}^{\#q \times \#q}$ and $U = \frac{\partial J^T f_c}{\partial u} \in \mathbb{R}^{\#q \times 6}$ have to be considered in order to properly take into account the initial contact force preload.

As described in [10], a rigid model of hand/object interaction does not allow the computation of the contact force distribution. The problem can be simply solved by introducing a *virtual spring* at the contact points. One extreme of each virtual spring is attached to the hand and the other to the object, both in the nominal contact location. The virtual spring model generates a force variation corresponding to the local interpenetration of the hand and object parts. Correspondingly, a contact force variation is described in (3) through the introduction of the *contact stiffness* matrix $K_c \in \mathbb{R}^{c \times c}$.

The basic grasp equations (1), (2) and (3) can be rearranged in matrix form as

$$\begin{bmatrix} I & 0 & G & 0 & 0 \\ 0 & I & -J^T & -Q & -U \\ 0 & 0 & I & -K_c J & K_c G^T \end{bmatrix} \begin{bmatrix} \delta w \\ \delta \tau \\ \delta f_c \\ \delta q \\ \delta u \end{bmatrix} = 0. \quad (6)$$

This is a linear homogeneous system of equations in the form $\Phi \delta \varphi = 0$, where $\Phi \in \mathbb{R}^{r_\Phi \times c_\Phi}$ is the coefficient matrix, and $\delta \varphi \in \mathbb{R}^{c_\Phi}$ is the vector containing all system variables. From (6), we easily obtain that Φ is always full row rank, and its dimensions are

$$\begin{aligned} r_\Phi &= \#w + \#q + \#f, \\ c_\Phi &= 2\#w + 2\#q + \#f. \end{aligned} \quad (7)$$

These facts imply that a basis for the solution space of the system has dimension $c_\Phi - r_\Phi = \#w + \#q$. Thus, a perturbed configuration of the system can be completely described knowing the values of the external wrench variation, δw , and the displacements of the joint configuration¹, δq . We will refer to these as the *independent variables* of the system. The *dependent variables* will be indicated as $\delta \varphi_d = [\delta \tau^T, \delta f_c^T, \delta u^T]^T$.

Acting on the coefficient matrix of the system, it is possible to obtain a formal method to get an explicit expression of the dependent variables of the system, as a function of the independent ones. This result is achievable extending the *elementary Gauss operations*, defined for typical linear systems of equations, in order to act on a block partitioned matrix. A general algorithm to obtain the desired form starting from (6), called GEROME-B, as completely described in Chapter 12. The final result of the procedure is a set of equations of the type

$$\delta \varphi_d = W_d \delta w_c + R_d \delta q, \quad (8)$$

where W_d and R_d are matrices of suitable dimensions. In the rest, we will mostly focus on the study of the controllability of grasping with different hand actuation systems, hence considering a null external wrench variation in (8). For the sake of completeness, we report here on the structure of this matrix, which can be partitioned as $R_d = [R_\tau^T \ R_f^T \ R_u^T]^T$, with the following explicit formulae

$$\begin{aligned} R_\tau &= Q + J^T K_c J + (U - J^T K_c G^T) (G K_c G^T)^{-1} G K_c J, \\ R_f &= K_c J - K_c G^T (G K_c G^T)^{-1} G K_c J, \\ R_u &= (G K_c G^T)^{-1} G K_c J. \end{aligned} \quad (9)$$

¹ From the previous considerations, it follows that other choices are possible. However, a complete discussion about these cases is out of the scope of this work.

2.2 Approaches to Simplification

Full independent actuation of the joints, in principle, offers the widest range of grasping and manipulation possibilities, limited only by the hand kinematics. As a counterpart, the large number of actuators needed causes complication in the design and a growth of the costs. Even disregarding the hardware aspects, however, the exploitation of the potential of full independent actuation requires sophisticated programming and control of the hand. Programming complexity turns often out to represent a major obstacle to usability and efficiency in real-world applications of robot hands.

Recently, researchers tried to find a trade off between the full utilization of the hand capabilities and the simplicity in control. Neuroscience studies, as widely described in Chapters 1-5, 9, 10, 14 and e.g. in [11, 12, 13], showed that humans control their hand by organized motion patterns or primitives. Particular muscular activation patterns produce correlated movements of the hand joints, which form a base set [14]. As extensively discussed in this book, especially in the first part (e.g. Chapter 1), such base is referred to as the space of the *postural synergies*, or *eigengrasp space* [15, 16, 17]. What makes the bio-aware synergy basis stand out among other possible choices for the basis to describe the hand configuration is the fact that most of the hand grasp posture variance, actually the 80%, is explained just by the first two synergies, and the 87% by the first three [18]. This renders the synergy space a credible candidate as a basis for simplification.

In order to transfer this concept in robotics, the *synergy matrix* $S \in \mathbb{R}^{\#q \times \#\sigma}$ is introduced, describing the principal components of a dataset of grasping postures, where $\#\sigma \leq \#q$ is the number of used synergies. With this actuation scheme, a hand configuration can be represented in the synergy space by the coordinate vector $\sigma \in \mathbb{R}^{\#\sigma}$ as

$$q = S\sigma. \quad (10)$$

A similar approach was used in [15], where *software synergies* were used to simulate a correlation pattern between joints of a fully actuated robotic hand. Software synergies can substantially simplify the design phase of a grasp, by reducing the number of control variables (see also [19]). However, software synergies clearly do not impact the simplification of the design of physical hands. The synergy concept was also applied via hardware, as in the design proposed in [20], where the authors used a train of pulleys of different radii to simultaneously transmit different motions to each joint.

Both the aforementioned software and hardware implementation of hand synergies assumed a model of the hand with a number of independent actuators (or Degrees of Actuation, DoAs) smaller than the number of joints (or Degrees of Freedom, DoFs). This causes the hand to move in a way that does not necessarily comply with the shape of an object to be grasped, hence resulting in few contacts being established between the hand and the object. To face this problem, some fixes can be considered, such as e.g. stopping the motion of each finger when it comes in contact with the grasped object, while prosecuting motion of others, or introducing a

complementary actuation system for modifying the shape of synergies. While these techniques can be considered to simplify the grasp approaching phase design, they do not benefit from synergy concept to control grasping forces.

2.3 Soft Synergies

To fully take advantage of the synergistic approach, avoiding the previously explained limitations, the idea of *soft synergies* was introduced and discussed in [2]. In this model, synergy coordinates define the configuration of a *virtual hand*, toward which the real one is attracted by an elastic field. To describe this situation, we introduce a *reference configuration* vector $q_r \in \mathbb{R}^{\#q}$, describing the configuration of the virtual hand. In this model, the motion of the virtual hand is directly controlled in the synergy space as

$$\delta q_r = S \delta \sigma. \quad (11)$$

The difference between the real position of the hand and its reference configuration generates the joint torques, which, at equilibrium, balance the interaction forces between the real hand and the grasped object. In formulae, defining a *joint stiffness* matrix $K_q^s \in \mathbb{R}^{\#q \times \#q}$, the joint torques in the soft synergy model are given by

$$\delta \tau = K_q^s (\delta q_r - \delta q). \quad (12)$$

By kineto-static duality, introducing the generalized force in the synergy space $\delta \varepsilon \in \mathbb{R}^{\#\sigma}$, we immediately get that

$$\delta \varepsilon = S^T \delta \tau. \quad (13)$$

One important aspect of the soft synergy model, is that it enables to reduce the number of degrees of actuation, while retaining all the kinematic degrees of freedom leaving the fine adjustment of the $\#q - \#\sigma$ remaining movements to the hand compliance. A conceptual hardware implementation of this idea is shown in fig. 2(b). This kind of underactuation scheme can be easily modeled by considering (11), (12) and (13), along with the grasp equation (8). In particular, for zero external wrenches on the object, for the joint torques it holds

$$\delta \tau = R_\tau \delta q, \quad (14)$$

where $R_\tau \in \mathbb{R}^{\#q \times \#q}$ was described in (9). Substituting (14) in (12), taking into account (11), we obtain

$$\delta q = (K_q^s + R_\tau)^{-1} K_q^s S \delta \sigma := H^s K_q^s S \delta \sigma. \quad (15)$$

Although the idea of soft synergy actuation sketched in fig. 2(b) appears to provide an elegant solution to the problem of simple hand design, merging the natural motion inherited from the postural synergy approach with adaptivity due

to compliance, its implementation in a mechanical design unfortunately turned out not to be very easy or practical, at least in our attempts.

2.4 Adaptive Synergies

A distinct thread of research work has addressed the design of simple robot hands via the use of a small number of actuators without decreasing the number of DOF. This approach, authoritatively described in [6], is referred to as *underactuation* and has produced a number of interesting hands since the earliest times of robotics. For further details the reader can refer to [21], [22], [23], and also to [24], [25], [26] and [27].

The basic idea enabling shape adaptation in underactuated hands is that of a differential transmission, the well-known mechanism used to distribute motion of a prime mover to two or more DOFs. Differentials can be realized in various forms, e.g. with gears [28], closed-chain mechanisms [28], or tendons and pulleys [29], and concatenated so as to distribute motion of a small number of motors to all finger joints q . Letting the vector $z \in \mathbb{R}^{\#z}$, with $\#z \leq \#q$, denote the position of the prime movers, a general differential mechanism is described by the kinematic equation

$$A\delta q = \delta z, \quad (16)$$

where $A \in \mathbb{R}^{\#z \times \#q}$ is the transmission matrix, whose element A_{ij} is the transmission ratio between the i^{th} actuator to the j^{th} joint. By kineto-static duality, the relationship between the actuation force vector $\eta \in \mathbb{R}^{\#z}$ and the joint torques is

$$\delta \tau = A^T \delta \eta. \quad (17)$$

The kinematic model (16) highlights the non-uniqueness of the position attained by an underactuated hand. Indeed, being the transmission matrix A a rectangular fat matrix, an infinity of possible hand postures δq exist which satisfy (16) for a given actuator position δz , their difference belonging to the kernel of A .

While these kernel motions are exactly those that provide underactuated hands with the desirable feature of *shape adaptivity*, in practice these hands associate to differential mechanisms the usage of passive elements such as mechanical limits, clutches, and springs [6]. Reasons for adding passive elements are various, including avoiding tendon slackness and ensuring the uniqueness of the position of the hand when not in contact with the object.

Let us define the model of an underactuated hand with elastic springs depicted in fig. 2(c) as *adaptive synergy* actuation. Notice that springs are arranged in parallel with the actuation and transmission mechanism, as opposed to the soft synergy model in fig. 2(b) where they are in series. Defining a joint stiffness matrix as $K_q^a \in \mathbb{R}^{\#q \times \#q}$, the balance equation (17) is rewritten as

$$\delta \tau = A^T \delta \eta - K_q^a \delta q. \quad (18)$$

Considering (18) and (14), it immediately follows that

$$\delta q = (K_q^a + R_\tau)^{-1} A^T \delta \eta := H^a A^T \delta \eta. \quad (19)$$

Thus, substituting this in (8), we obtain a description of the hand/object equilibria caused by the application of given actuator forces.

If instead actuators are modelled as position sources, by substituting equation (19) in (16) and inverting, we find

$$\delta \eta = (A H^a A^T)^{-1} \delta z. \quad (20)$$

Substituting this result in (19), we then obtain

$$\delta q = H^a A^T (A H^a A^T)^{-1} \delta z. \quad (21)$$

Finally, a complete system description in the case of actuator position control is given by substituting (21) in (8).

2.5 From Soft to Adaptive Synergies

Summarizing the discussion so far, we have seen that two design techniques, i.e. *soft* and *adaptive* synergies, for multiarticulated hands with simple mechanics stand out for different reasons. Soft synergies provide a robust theoretical basis for the design of anthropomorphic hands but without an effective technological implementation. On the contrary, under-actuated hands (adaptive synergies) can be developed exploiting simple elements, such as differential and elastic ones.

For this reason, assuming that a desired soft synergy model is assigned through its synergy and stiffness matrices, S and K_q^s respectively, our goal is to find a corresponding adaptive synergy model, identified by a transmission matrix A and a joint stiffness K_q^a , which exhibits the same behavior, at least locally, around an equilibrium configuration.

As shown in the previous Sections, the behavior of the hand/object system is slightly different if the hand is position controlled or force controlled. This holds true for both soft and adaptive synergy model. Nevertheless, in all of the cases, the system is described as a linear map from an independent variable $\delta \varphi_i$, that can be $\delta \sigma$ or δz , and the joint displacement as $\delta q = \Phi_i \delta \varphi_i$, where Φ_i is taken from one of (15) or (21), respectively. By means of (8), the joint displacement describes the variation of the dependent variables at the hand/object level.

The map can be also defined in the opposite direction, starting from a given adaptive synergy, to obtain a corresponding soft synergy. The total amount of possible maps is eight, considering both the case of position and force control.

We will describe now the procedure to find one of such mappings, from a given position controlled soft synergy model to the corresponding position controlled adaptive synergy hand. All the other maps can be found with similar procedures.

The hand/object behavior for a position controlled soft synergy hand is defined by (15), while the behavior of an adaptive underactuated hand is controlled by (21). To match them means to impose

$$H^s K_q^s S \delta \sigma = H^a A^T (A H^a A^T)^{-1} \delta z. \quad (22)$$

Looking at the span of the second term of the previous equation, it is possible to see that

$$\text{span} \left\{ H^a A^T (A H^a A^T)^{-1} \right\} = \text{span} \{ H^a A^T \}, \quad (23)$$

since the term $(A H^a A^T)^{-1}$ is a square full rank matrix. As a consequence, the span of the two terms in (22) can be matched by imposing

$$H^a A^T = H^s K_q^s S M, \quad (24)$$

where matrix M can be any full rank square matrix of suitable dimensions, which can be used as design parameter and accounts also for measurement units harmonization. Given the choice on (24), a suitable relationship from $\delta \sigma$ to δz can be found in the form

$$\delta z = (A H^a A^T) M^{-1} \delta \sigma, \quad (25)$$

completing the map between the two actuation systems.

3 The Pisa/IIT SoftHand

In this section we apply the adaptive synergy design approach previously described and depicted in fig. 2(c) to the design of a humanoid hand. The hand was designed according to few specifications. On the functional side, the main requirement is the capability of grasping as wide a variety of objects and tools as possible, among those commonly used by humans in everyday tasks. The hand should be primarily able to execute *whole hand grasp* of tools, properly and strongly enough to operate them under arm and wrist control, but it should also be able to achieve *tip grasps*. No in-hand dexterous manipulation is required for this prototype. The main nonfunctional requirements are resilience against force, overexertion and impacts, and safety in interactions with humans. The hand should be lightweight and self-contained, to avoid encumbering the forearm and wrist with motors, batteries and cabling, along with cost effectiveness.

In order to meet the first functional requirement, the hand was designed anthropomorphically, with 19 DOFs arranged in four fingers and an opposable thumb (fig. 3(a)). To maximize simplicity and usability, however, the hand uses only one actuator. According to our design approach, the motor actuates the adaptive

synergy as derived from a human postural database, see also Chapters 1, 2, 4 and 14. The mechanical implementation of the first soft synergy through shape-adaptive underactuation was obtained via the numerical evaluation of the corresponding transmission matrix R and joint stiffness matrix K_q^a appearing in (16) and (18).

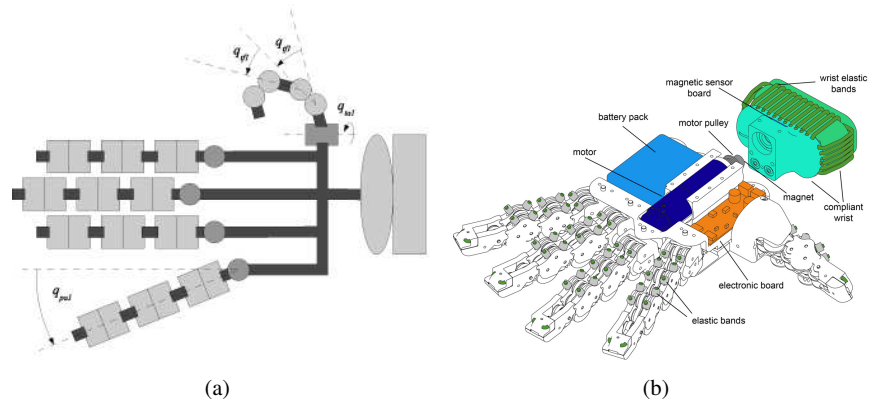


Fig. 3: Panel (a) shows the kinematics of the Pisa/IIT SoftHand. Revolute joints are in dark gray, while rolling-contact joints are in light gray. In panel (b), a three-dimensional view of the Pisa/IIT SoftHand. Main components (the motor, the battery pack and the electronic control board), joints and wrist architecture are highlighted.

The hand assembly design is shown in fig. 3(b). Each finger has four phalanges, while the thumb has three. The hand palm is connected to a flange, to be fixed at the forearm, through a compliant wrist allowing for three passively compliant DOFs.

The wrist of the SoftHand is composed by two curved surfaces, able to roll one on the other. The contact between them is guaranteed by the use of elastic ligaments, arranged along the perimeter of the wrist. When relative motion of the surfaces arises, for example caused by an external load, a set of elastic forces appears. The wrist comes back to the original configuration when the external load is removed.

In rest position, with fingers stretched out and at a relative angle of about 15° in the dorsal plane, the hand spans approximately 230 mm from thumb to little finger tip, is 235 mm long from the wrist basis to the middle finger tip and has 40 mm maximum thickness at the palm. The weight of the hand is approximately 0.5 kg. The requirement on power grasp implies that the hand is able to generate a high enough grasping force, and to distribute it evenly through all contacts, be them at the fingertips, the inner phalanges, or the palm. These goals are naturally facilitated by the shape adaptivity of the soft synergy approach, yet they also require strong enough actuation and, very importantly, low friction in the joints and transmission mechanisms.

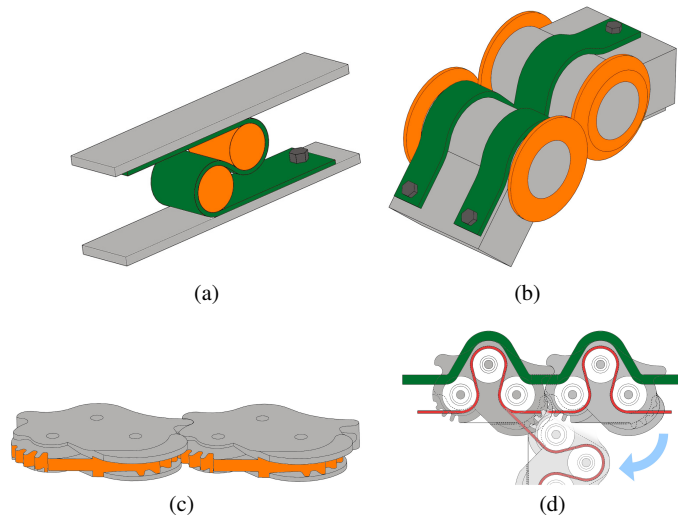


Fig. 4: Schematic illustration of two examples of COMPLIANT Rolling-contacts Elements (CORE): a Rolamite joint (a) and a Hillberry joint (b). Design of the compliant rolling-contact joint used in the interphalangeal joints of the Pisa/IIT SoftHands: (c) perspective view with rolling cylinders with matching multi-stable profile; (d) lateral view, showing the arrangement of ligaments and tendons.

The requirement on resilience and safety was one of the most exacting demands we set out for our design, as we believe these to be crucial features that robots must possess to be of real use in interaction with, and assistance to, humans. This is only more true for hands, the body part primarily devoted to physical interaction with the environment for exploration and manipulation. To achieve this goal, we adopted a non-conventional “soft robotics” design of the mechanics of the hand, that fully exploits the potential of modern material deposition techniques to build a rather sophisticated design with rolling joints and elastic ligaments at very low cost. A first departure from conventional design is the use of rolling contact articulations to replace standard revolute joints. Our design takes inspiration from a class of joints known as COMPLIANT Rolling-contact Elements (CORE) [30, 31], aka “Rolamite” or “XRjoints” joints [32] (see fig. 4(a)). Among these, Hillberry’s design of a rolling joint [33] is particularly interesting to our purposes.

A Hillberry joint consists of a pair of cylinders in rolling contact on each other, held together by metallic bands, which wrap around the cylinders on opposite sides as schematically shown in fig. 4(a). In Hillberry joints (see fig. 4(b)), the band arrangement results in a compliant behavior in flexion but rigid in traction. The joint forms a higher kinematic pair, whose motion is defined by the profile of the cylinders, and exhibits very low friction and abrasive wear. The joint behaves more similarly to the human articulation than simple

revolute joint, and for this reason was originally proposed for knee prostheses [33]. Hillberry joints have been used in few robotic applications before, including robot hands [34]. Fig. 3(a) shows how we used CORE joints in the design of the Pisa/IIT SoftHand. In particular, we adopted CORE joints for all the interphalangeal, flexion/extension articulations. Conversely, conventional revolute joints were used for metacarpo-phalangeal, abduction/adduction articulations. Our design introduces a few important modifications of existing rolling–contact joints, which are illustrated in fig. 4(c) and 4(d). Firstly, metallic bands were replaced by elastic ligaments, realized a polyurethane rubber able to withstand large deformations and fatigue, and are fixed across the joint with an offset in the dorsal direction. Suitable pretensioning of the ligaments, together with a carefully designed profile of the two cylinders, introduces a desirable passive stability behavior, with an attractive equilibrium at the rest configuration with fingers stretched. The elastic ligaments are polyurethane rubber segments of 2 mm diameter, characterized by 88 Shore A hardness. The rest length of the ligaments is 10 mm. Some pre-tensioning is applied with a stretch in the range between 2 to 5 mm. All the long fingers proximal flexion joints have lower values of pre-tensioning, with respect to all the other joints, in order to guarantee a hand motion similar to the first human postural synergy (see Chapters 1 and 3), as explained in Section 2.4.

The coupled rolling cam profiles are designed on a circular primitive with radius 6.5 mm. The actuation tendon is wrapped around pulleys with radius 3.5 mm. All the radii are the same for all the rolling profiles and the pulleys, in order to obtain a modular design. The rolling cam profile is realized on cylinder portions flanked by lateral walls on both sides, whose slope is about 80° (see fig. 4(c), 4(d) and fig. 6). When two phalanges are assembled, such walls are housed in a fitting recess of the matching phalanx. These features of our design are particularly important for the system to behave softly and safely at contact, and to recover from force overexertion, due e.g. to impacts or jamming of the hand, making the hand automatically return to its correct assembly configuration. Indeed, these joint can withstand severe disarticulations (cfr. fig. 6) and violent impacts (fig. 7).

The design of interphalangeal joints does not require the use of screws, shafts, bearings or gears. As it can be seen in fig. 4(c) and 4(d), a few teeth of an involute gear of vanishing height are indeed integrated in the cam shape, to better support tangential loads at the joint.

Actuation of the hand is implemented through a single Dyneema tendon routed through all joints using passive anti-derailment pulleys. The tendon action flexes and adducts fingers and thumb, counteracting the elastic force of ligaments, and implementing adaptive underactuation without the need for differential gears (fig. 5).

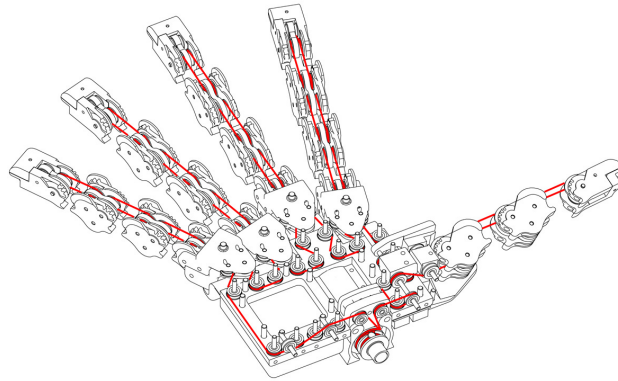


Fig. 5: Partially exploded line sketch of the Pisa/IIT SoftHand. The tendon routing distributes the motion to all joints.

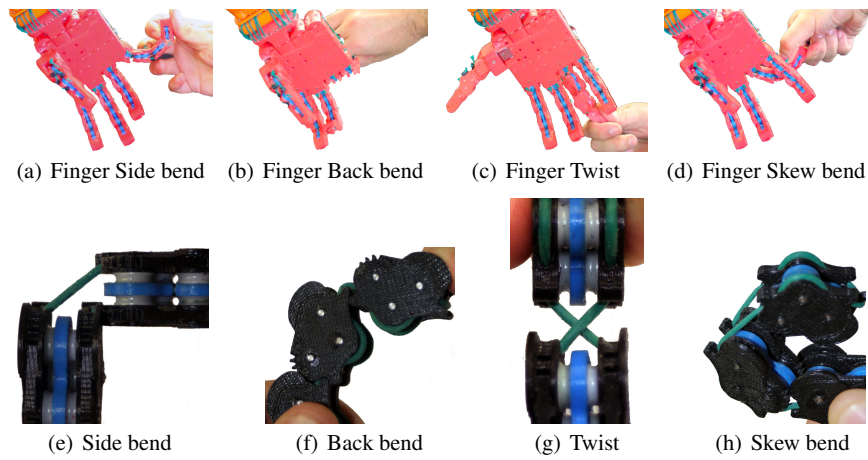


Fig. 6: The Pisa/IIT SoftHand joints can withstand severe force overexertion in all directions, automatically returning to the correct assembly configuration.

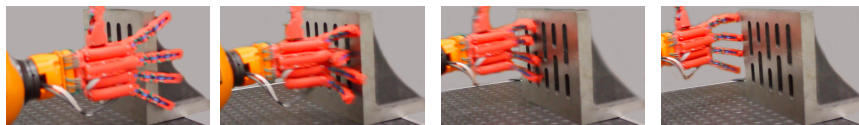


Fig. 7: A photo-sequence showing the PISA/IIT SoftHand during a violent impact with a stiff surface.

4 Experimental Results

The prototype of the Pisa/IIT SoftHand (fig. 1) was built to perform experimentally tests. The actuator powering the hand is a 6 W Maxon motor RE-max21 with a reduction ratio of 84:1 equipped with a 12 bit magnetic encoder (Austrian Microsystems AS5045) with a resolution of 0.0875° .

The embedded electronic unit hosting sensor processing, motor control and communication is located in the hand back, along with the battery pack. The opening/closing of the hand is controlled via a single set point reference, communicated via one of the available buses (SPI and RS-485).

During experiments the hand worn an off-the-shelf working glove with padded rubber surfaces, supplying contact compliance and grip.

4.1 Force and torque measurements

An interface equipped with an ATI nano 17 F/T sensor was used to measure the holding force and torque of the robotic hand. In the first case, a split cylinders, represented in fig. 8(a), was used to measure the grasp force. The cylinder is 120 mm high and has a diameter of 45 mm. The disk to measure maximum holding torque is represented in fig. 8(b). The disk is 20 mm high and has a diameter of 95 mm.

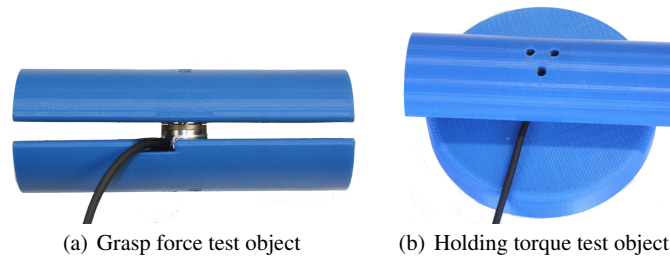


Fig. 8: Sensorized object for force measurements (a), sensorized object for torque measurements (b).

In fig. 9(b) we report force acquisitions while the hand grasped the sensorized object. It is possible to notice how forces increased when fingers get in contact with the sensorized cylinder (step behavior of the lines in fig. 9(b)). We achieved a maximum holding torque of 2 Nm and maximum holding force of about 20 N along the z axis. These limits appear to be dictated by the motor size rather than by the hand construction. Although we did not go through an exhaustive analysis, in an occasional experiment with a stronger motor, we obtained holding torque of 3.5 Nm and holding force of 28 N.

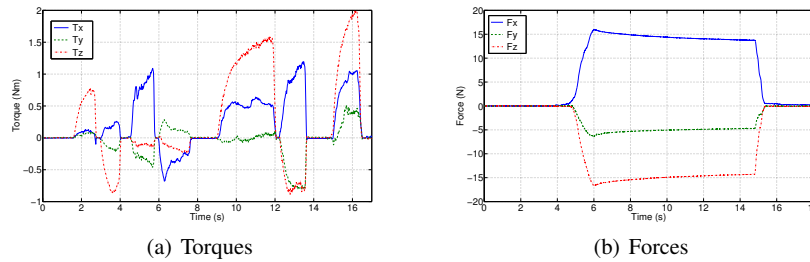


Fig. 9: Torques and forces of the robotic hand during grasp task.

4.2 Grasp Experiments

To test the adaptiveness of the robotic hand, the grasp of several objects of daily use in a domestic or lab environment were performed. Grasp experiments were performed in three different conditions: 1) the hand wrist fixed on a table and the object placed in the grasp; 2) the object placed on a table and the hand mounted on a robot arm, and 3) the hand wrist fixed to the forearm of a human operator.

Some examples of grasps achieved in the first condition are reported in fig. 10.

To test usage of the Pisa/IIT SoftHand in a robotic scenario, the hand was mounted at the end-effector flange of a KUKA Light-Weight robot arm. Fig. 11 shows some of the grasps tested. Notice that the robot was manually programmed to reach an area where the object was approximately known to lie, and no grasp planning phase was executed. Rather, the hand was given a closure command by software. The closure time, as well as the robot trajectory, were preprogrammed in the examples shown, and were the same for each object lying roughly in the same area.

Finally, to test the capability of the Pisa/IIT SoftHand to acquire complex grasps of objects randomly placed in the environment, we developed a wearable mechanical interface (see fig. 12) allowing an operator to use our hand as a substitution of his/her own. The interface can be strapped on the operator's forearm and can be controlled by the operator acting on a lever with his/her real hand (see fig. 12(a)). In fig. 13 we report some grasps executed with the human interface (condition 2 above). In summary, a total of 107 objects of different shape was successfully grasped, with a whole hand or a tip grasp, in all conditions previous considered, during our tests: bottle, reel, pincer, stapler, pen, phone handset, plier, teddy bear, cup, handle, spray, computer mice, hot-glue gun, human hand, cell phone, glass, screw-driver, hammer, file, book, coin, scotch tape holder, ball, tea bag, ketchup bottle, hamburger, camera, tripod stand, cutter, trash can, keyboard, torch, battery container, battery (AA), small cup, measuring tape, caliper, wrench, lighter, eraser, world map (globe), remote control, hex key, AC adapter, keyring, spoon, fork, knife, hand tissue box, liquid soap dispenser, corkscrew, rag, candy, calculator, slice of cake, rubber-stamp, spring, paper, cellphone case, rubber band,

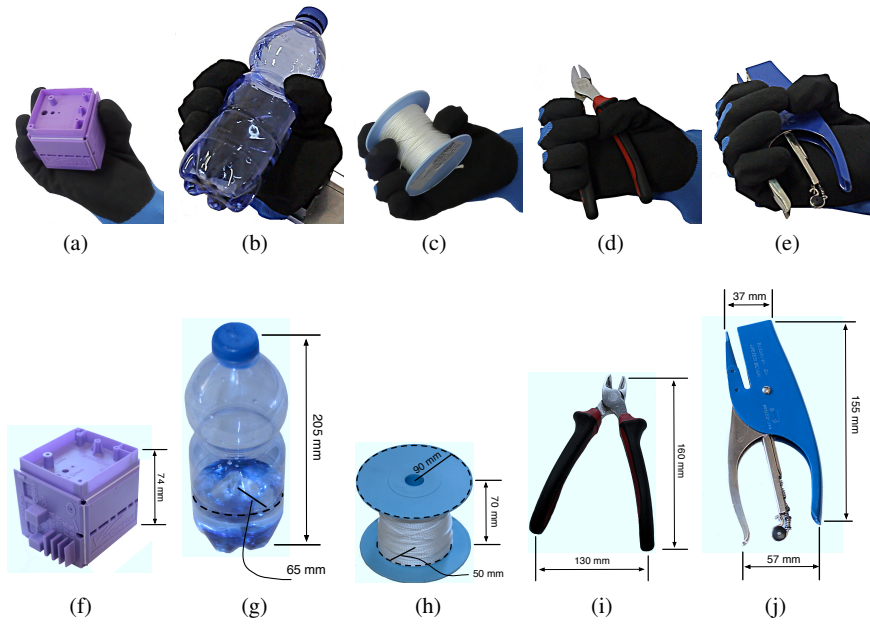


Fig. 10: Some experimental grasps performed with the Pisa/IIT SoftHand, with the object placed in the hand by a human operator.

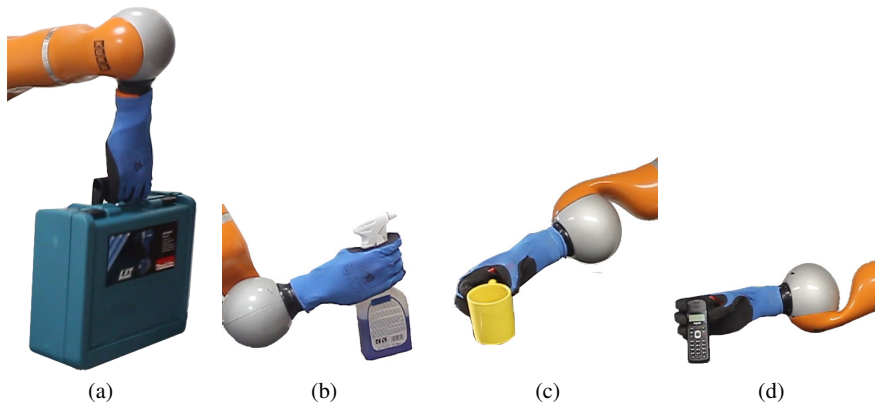


Fig. 11: Grasps executed with the Pisa/IIT SoftHand mounted on a Kuka Light Weight Robot: handbag (a), spray (b), cup (c) and telephone (d).

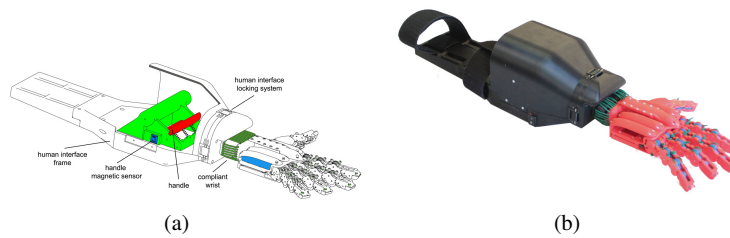


Fig. 12: (a) Components of the interface for human use of the Pisa/IIT SoftHand. The angle position of the lever is adopted as reference position to drive the actuator of the hand. (b) Appearance of the assembled human interface prototype.

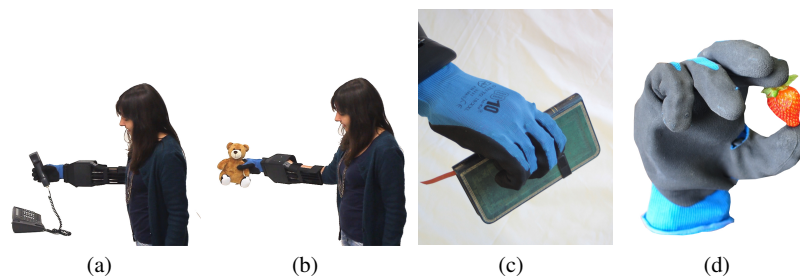


Fig. 13: Some examples of grasps executed with the robotic hand mounted on a wearable Human Robot Interface: telephone (a), Teddy Bear (b), book (c), and strawberry (d).

bottle top, watch, umbrella, broom, garbage scoop, scarf, chair, schoolbag, USB cable, glue stick, wallet, credit card, sponge, pencil sharpener, straight edge, safety lock, mouse pad, hard disk, jacket, drill, chalk, notebook, blackboard eraser, door lock, square ruler, scissors, eyeglasses, deodorant, USB key, hat, headphones, cigarette, helmet, screw (M8), clamp, fridge magnet, drill bit, table calendar, saw, tape cassette, beauty case, bubble gum box, bubble gum, tissue pocket, dish, poster.

The more difficult situation is in grasping very thin objects. However, since grasp limitations of the prototype are also influenced by the operator training, it is not easy to quantify grasp limitations without resorting to further investigations on operator's capabilities, which are out of the scope of this paper.

5 A New Set of Possibilities

One of the main lessons learned through these experiments is that, while all grasps could be easily achieved by the hand when operated by a human, programming the robot to achieve the same grasps was in some cases rather

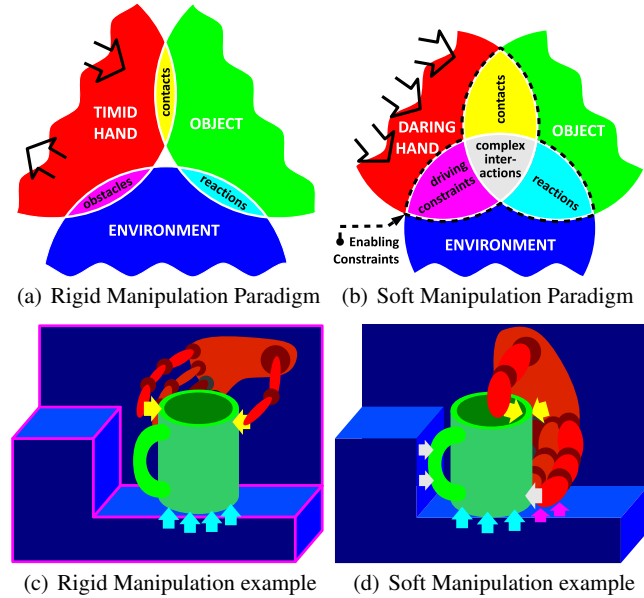


Fig. 14: Paradigm shift in manipulation, from rigid manipulation (left) to soft manipulation (right). Primary colors identify the scenario main actors: red for the robotic hand, blue for the environment, green for the target object. Secondary colors codify simple interactions between the actors: yellow for hand-object, cyan for object-environment and magenta for environment-hand. Finally, complex interactions, which involve all the three actors at the same time, are white colored.

complex. One of the main reason for this is, in our understanding, that the human operator quickly learns how to exploit the intrinsic adaptivity of the hand, including the wrist compliance, to shape the hand before and during grasp. This is done with the help of object features and/or environmental constraints, notably the table top and walls. This observation hints that autonomous learning and planning for soft robot grasping might have to be focused on constraint-based motion rather than on free-space, multi-DOF hand shaping. This kind of features allow to use these hands in more “daring” interactions with the objects and the environment, in contrast with the “timid” approach typically adopted with rigid hands. In fact, Soft Hands can use their full surface for enveloping grasps, and exploiting objects and environmental constraints, in order to functionally shape themselves, going beyond their nominal kinematic limits by exploiting structural softness.

The differences between a rigid and soft approach to manipulation are sketched in Fig. 14. In the classical paradigm (cfr. fig. 14(a)), the planner searches for suitable points on the object that generate a nominal grasp of good quality, and for trajectories that can bring there the fingertips while avoiding contacts of the hand with the environment. In the example of fig. 14(c), to grasp the green cup while

avoiding the wall on the left the planner has to find a path in a narrow passage. However, soft manipulation subverts this scheme (fig. 14(b)). In the example of fig. 14(d), hand-object, object-environment and hand-environment contacts are not avoided but rather sought after and exploited to shape the hand itself around the object.

The set of all possible physical interactions between the hand, the object and the environment, which define the hand-object functional interaction, will be referred to as the set of *Enabling Constraints*. The analysis of such possibilities constitute a rather new challenge for existing grasping algorithms: adaptation to totally or partially unknown scenes remains a difficult task, toward which only some approaches have been investigated so far. Some of them are model-free and propose geometrical features which indicate good grasps [35, 36], some others evaluate also topological object properties such as holes [37]. Typically, grasps are ranked on a fixed list of suitable hypotheses, do not require supervised learning, but do not adapt over time. Other methods are based on learning the success rate of grasps given some descriptor extracted from sensor data, either evaluated on a real robotic system [38, 39], or on simulated sensor data [40, 41].

Moreover, beside vision-based methods, hand compliance offers the real possibility to use tactile exploration for 3D reconstruction of unknown environments and objects. Indeed, tactile sensing can solve some severe limitations of computer vision, such as sensitivity to illumination and limited perspective. As an example, a combined procedure based on dynamic potential fields, that aims at reconstructing 3D object models, which are then used for grasp planning and execution was presented in [42] and recently extended in [43].



Fig. 15: A human hand grasping a cup with three different approaches (top panels) and the same grasps reproduced with the Pisa/IIT SoftHand (bottom panels).

An important observation from the way humans use their real hands is that, in everyday grasping and manipulation tasks, the role of hand compliance is fundamental. In the first place it is used to adapt to the shape of the hand surroundings: both the target object and the rest of the environment. On the other hand, it is important to notice how the objects and the environment constraints are used, in turn, to functionally shape the hand, going beyond its nominal kinematic limits by exploiting its structural softness.



Fig. 16: The Pisa/IIT SoftHand mounted on a human arm.

Although one could ascribe such levels of dexterity to the high levels of sensory-motor capabilities of the human hand itself, it is astounding to compare the performance of the human naked hand with that of a person using a simple robot hand, as the Pisa/IIT SoftHand arm-mounted device shown in Fig. 16.

Thanks to its under-actuated mechanisms the SoftHand is capable to grasp several number of objects by matching to their shape. These combination of simplicity, adaptivity and robustness lets the person experiment in a very natural way with the robotic hand, and soon achieve a level of performance comparable, often similar, to that obtained with their true hands. This achievement is obtained despite the presence of just one degree of actuation on the mechanism and an almost total lack of tactile feedback, and has encouraged the exploitation of the Pisa/IIT SoftHand as an ideal platform for the development of a novel hand prosthesis, as described in Chapter 9. Fig. 15, shows three very different ways to grasp a cup, implemented with both the bare human hand and the SoftHand.

Notice that the SoftHand can substantially match the grasping performance of the human hand thanks to its possibility of exploring and exploiting the *Enabling Constraints* that define, at a very basal level, the problem of grasping and manipulation.

As a further example, consider Fig.s 17, where the combined action of adaptability and robustness allow the user to manipulate and interact with both the environment and the object at the same time, in a complex way (refer also to Fig. 14). Exploiting all the physical constraints that are external with respect to the hand itself: walls, surfaces and edges, force closures of the object between the



Fig. 17: A person with the arm-mounted SoftHand can seamlessly execute also difficult manipulation tasks which involve combined interactions between hand, object and environment.

hand and the environment can be obtained and used to generate simple and effective manipulation tasks, in this case sliding and pivoting a book.

6 Conclusion

This Chapter presented the design and implementation of the Pisa/IIT SoftHand, along with the theoretical framework behind that justifies the main design choices. The important aspect of the hand actuation pattern is considered first, reviewing various past and recent approaches, and finally considering adaptive synergies as preferred choice.

The first prototype of the Pisa/IIT SoftHand, a highly integrated robot hand characterized by a humanoid shape and good robustness and compliance, is presented and discussed. The hand is validated experimentally through extensive grasp cases and grasp force measurements. Finally considerations on new sets of possibilities were shown, discussing the possibility of a paradigm shift in manipulation approaches, from rigid to soft manipulation, with further developments toward prosthetics, as discussed in Chapter 9.

Acknowledgments

The authors would like to thank Andrea Di Basco, Fabrizio Vivaldi, Simone Tono and Emanuele Silvestro for their valuable help in the realization of the prototypes.

This work was supported by the European Commission under the CP-IP grant no. 248587 “THE Hand Embodied”, within the FP7-2007-2013 program “Cognitive Systems and Robotics”, the grant no. 645599 “SOMA: Soft-bodied Intelligence for Manipulation”, funded under H2020-EU-2115, the ERC Advanced Grant no. 291166 “SoftHands: A Theory of Soft Synergies for a New Generation of Artificial Hands”.

References

- [1] M. Gabbicini, A. Bicchi, D. Prattichizzo, and M. Malvezzi, “On the role of hand synergies in the optimal choice of grasping forces,” *Autonomous Robots*, vol. 31, no. 2 - 3, pp. 235 – 252, 2011.
- [2] A. Bicchi, M. Gabbicini, and M. Santello, “Modelling natural and artificial hands with synergies,” *Philosophical Transactions of the Royal Society B: Biological Sciences*, vol. 366, no. 1581, pp. 3153–3161, 2011.
- [3] M. G. Catalano, G. Grioli, A. Serio, E. Farnioli, C. Piazza, and A. Bicchi, “Adaptive synergies for a humanoid robot hand,” in *IEEE-RAS International Conference on Humanoid Robots*, (Osaka, Japan), 2012.
- [4] M. G. Catalano, G. Grioli, E. Farnioli, A. Serio, C. Piazza, and A. Bicchi, “Adaptive synergies for the design and control of the pisa/iit soft hand,” *International Journal of Robotics Research*, vol. 33, p. 768–782, 2014.
- [5] M. Bonilla, E. Farnioli, C. Piazza, M. G. Catalano, G. Grioli, M. Garabini, M. Gabbicini, and A. Bicchi, “Grasping with soft hands,” in *International Conference on Humanoid Robots IEEE-RAS 2014*, (Madrid, Spain, November 18 - 20), In Press.
- [6] L. Birglen, C. Gosselin, and T. Laliberté, *Underactuated robotic hands*, vol. 40. Springer Verlag, 2008.
- [7] M. Gabbicini, E. Farnioli, and A. Bicchi, “Grasp and manipulation analysis for synergistic underactuated hands under general loading conditions,” in *Robotics and Automation (ICRA), 2012 IEEE International Conference on*, pp. 2836–2842, IEEE, 2012.
- [8] M. Gabbicini, E. Farnioli, and A. Bicchi, “Grasp analysis tools for synergistic underactuated robotic hands,” *International Journal of Robotic Research*, vol. 32, pp. 1553 – 1576, 11/2013 2013.
- [9] E. Farnioli, M. Gabbicini, M. Bonilla, and A. Bicchi, “Grasp compliance regulation in synergistically controlled robotic hands with vsa,” in *IEEE/RSJ International Conference on Intelligent Robots and Systems, IROS 2013*, (Tokyo, Japan), pp. 3015 –3022, November 3-7 2013.

- [10] A. Bicchi, "On the problem of decomposing grasp and manipulation forces in multiple whole-limb manipulation," *Int. Journal of Robotics and Autonomous Systems*, vol. 13, pp. 127–147, 1994.
- [11] E. J. Weiss and M. Flanders, "Muscular and postural synergies of the human hand.," *Journal of neurophysiology*, vol. 92, pp. 523–35, July 2004.
- [12] M. Santello, G. Baud-Bovy, and E. Joerntell, "Neural bases of hand synergies." note: in review, 2013.
- [13] C. Castellini and P. van der Smagt, "Evidence of muscle synergies during human grasping," *Biological Cybernetics*, vol. 107, pp. 233–245, April 2013.
- [14] T. Easton, "On the normal use of reflexes: The hypothesis that reflexes form the basic language of the motor program permits simple, flexible specifications of voluntary movements and allows fruitful speculation," *American Scientist*, vol. 60, no. 5, pp. 591–599, 1972.
- [15] M. Ciocarlie, C. Goldfeder, and P. Allen, "Dexterous grasping via eigengrasps: A low-dimensional approach to a high-complexity problem," in *Proceedings of the Robotics: Science & Systems 2007 Workshop-Sensing and Adapting to the Real World, Electronically published*, Citeseer, 2007.
- [16] D. Prattichizzo, M. Malvezzi, and A. Bicchi, "On motion and force controllability of grasping hands with postural synergies," *Proceedings of Robotics: Science and Systems, Zaragoza, Spain*, 2010.
- [17] T. Wimboeck, J. Reinecke, and M. Chalon, "Derivation and verification of synergy coordinates for the dlr hand arm system.," in *CASE*, pp. 454–460, IEEE, 2012.
- [18] M. Santello, M. Flanders, and J. Soechting, "Postural hand synergies for tool use," *The Journal of Neuroscience*, vol. 18, no. 23, pp. 10105–10115, 1998.
- [19] F. Ficuciello, G. Palli, C. Melchiorri, and B. Siciliano, "Experimental evaluation of postural synergies during reach to grasp with the ub hand iv," in *Intelligent Robots and Systems (IROS), 2011 IEEE/RSJ International Conference on*, pp. 1775–1780, IEEE, 2011.
- [20] C. Brown and H. Asada, "Inter-finger coordination and postural synergies in robot hands via mechanical implementation of principal components analysis," in *Intelligent Robots and Systems, 2007. IROS 2007. IEEE/RSJ International Conference on*, pp. 2877–2882, IEEE, 2007.
- [21] R. Tomovic and G. Boni, "An adaptive artificial hand," *Automatic Control, IRE Transactions on*, vol. 7, no. 3, pp. 3–10, 1962.
- [22] S. Hirose and Y. Umetani, "The development of soft gripper for the versatile robot hand," *Mechanism and machine theory*, vol. 13, no. 3, pp. 351–359, 1978.
- [23] A. Rovetta, "On functionality of a new mechanical hand," *Journal of Mechanical Design*, vol. 103, p. 277, 1981.
- [24] T. Laliberté and C. Gosselin, "Simulation and design of underactuated mechanical hands," *Mechanism and Machine Theory*, vol. 33, no. 1, pp. 39–57, 1998.
- [25] M. Carrozza, C. Suppo, F. Sebastiani, B. Massa, F. Vecchi, R. Lazzarini, M. Cutkosky, and P. Dario, "The spring hand: development of a self-adaptive

- prosthesis for restoring natural grasping,” *Autonomous Robots*, vol. 16, no. 2, pp. 125–141, 2004.
- [26] C. Gosselin, F. Pelletier, and T. Laliberte, “An anthropomorphic underactuated robotic hand with 15 dofs and a single actuator,” in *Robotics and Automation, 2008. ICRA 2008. IEEE International Conference on*, pp. 749–754, 2008.
- [27] A. Dollar and R. Howe, “The highly adaptive sdm hand: Design and performance evaluation,” *The International Journal of Robotics Research*, vol. 29, no. 5, p. 585, 2010.
- [28] T. Laliberte, L. Birglen, and C. Gosselin, “Underactuation in robotic grasping hands,” *Machine Intelligence & Robotic Control*, vol. 4, no. 3, pp. 1–11, 2002.
- [29] S. Hirose, “Connected differential mechanism and its applications,” *Proc. 2nd ICAR*, pp. 319–326, 1985.
- [30] J. R. Cannon and L. L. Howell, “A compliant contact-aided revolute joint,” *Mechanism and Machine Theory*, vol. 40, pp. 1273–1293, 2005.
- [31] A. Jeanneau, J. Herder, T. Laliberté, and C. Gosselin, “A compliant rolling contact joint and its application in a 3-dof planar parallel mechanism with kinematic analysis,” *ASME Conference Proceedings*, vol. 2004, no. 46954, pp. 689–698, 2004.
- [32] R. Cadman, “Rolamite - geometry and force analysis,” tech. rep., Sandia Laboratories, April 1970.
- [33] B. Hillberry and A. Hall Jr, “Rolling contact joint,” Jan. 13 1976. US Patent 3,932,045.
- [34] C. Ruoff, “Rolling contact robot joint,” Dec. 17 1985. US Patent 4,558,911.
- [35] K. Hsiao, S. Chitta, M. Ciocarlie, and E. G. Jones, “Contact-reactive grasping of objects with partial shape information,” in *Intelligent Robots and Systems (IROS), 2010 IEEE/RSJ International Conference on*, pp. 1–8, 2010.
- [36] E. Klingbeil, D. Rao, B. Carpenter, V. Ganapathi, A. Y. Ng, and O. Khatib, “Grasping with application to an autonomous checkout robot,” *2011 IEEE International Conference on Robotics and Automation*, pp. 2837–2844, May 2011.
- [37] F. T. Pokorny, J. A. Stork, and D. Kragic, “Grasping objects with holes: A topological approach,” *Proceedings - IEEE International Conference on Robotics and Automation*, pp. 1100–1107, 2012.
- [38] L. Montesano, M. Lopes, A. Bernardino, J. Santos-Victor, F. S. Melo, and R. Martinez-Cantin, “Learning grasping affordances from local visual descriptors,” in *Development and Learning, 2009. ICDL 2009. IEEE 8th International Conference on*, pp. 1–6, 2009.
- [39] R. Detry, E. Başeski, M. Popović, and Y. Touati, “Learning continuous grasp affordances by sensorimotor exploration,” *From motor learning to*, Jan. 2010.
- [40] J. Bohg and D. Kragic, “Learning grasping points with shape context,” *Robotics and Autonomous Systems*, vol. 58, pp. 362–377, Apr. 2010.
- [41] A. Saxena, J. Driemeyer, and A. Y. Ng, “Robotic Grasping of Novel Objects using Vision,” *The International Journal of Robotics Research*, vol. 27, pp. 157–173, Feb. 2008.

- [42] A. Bierbaum and M. Rambow, "Grasp affordances from multi-fingered tactile exploration using dynamic potential fields," *Humanoid Robots*, Jan. 2009.
- [43] A. Herzog, P. Pastor, M. Kalakrishnan, L. Righetti, J. Bohg, T. Asfour, and S. Schaal, "Learning of grasp selection based on shape-templates," *Autonomous Robots*, vol. 36, no. 1-2, pp. 51–65, 2013.